Printed 10/1/99
Submitted to Appl. Spectros.
99-2564J

Multi-window Classical Least Squares Multivariate Calibration Methods for Quantitative ICP-AES Analyses*

David M. Haaland, William B. Chambers, Michael R. Keenan, and

David K. Melgaard

Sandia National Laboratories

Albuquerque, NM 87185-0342

ABSTRACT

The advent of inductively coupled plasma-atomic emission spectrometers (ICP-AES) equipped with charge-coupled-device (CCD) detector arrays allows the application of multivariate calibration methods to the quantitative analysis of spectral data. We have applied classical least squares (CLS) methods to the analysis of a variety of samples containing up to 12 elements plus an internal standard. The elements included in the calibration models were Ag, Al, As, Au, Cd, Cr, Cu, Fe, Ni, Pb, Pd, and Se. By performing the CLS analysis separately in each of 46 spectral windows and by pooling the CLS concentration results for each element in all windows in a statistically efficient manner, we have been able to significantly improve the accuracy and precision of the ICP-AES analyses relative to the univariate and single-window multivariate methods supplied with the spectrometer. This new multi-window CLS (MWCLS) approach simplifies the analyses by providing a single concentration determination for each element from all spectral windows. Thus, the analyst does not have to perform the tedious task of reviewing the results from each window in an attempt to decide the correct value among discrepant analyses in one or more windows for each element. Furthermore, it is not necessary to construct a spectral correction model for each window prior to calibration and analysis. When

DISCLAIMER

DISCLAIMER

Portions of this document may be illegible in electronic image products. Images are produced from the best available original document.

one or more interfering elements was present, the new MWCLS method was able to reduce prediction errors for a selected analyte by more than 2 orders of magnitude compared to the worst case single-window multivariate and univariate predictions. The MWCLS detection limits in the presence of multiple interferences are 15 ng/g (i.e., 15 ppb) or better for each element. In addition, errors with the new method are only slightly inflated when only a single target element is included in the calibration (i.e., knowledge of all other elements is excluded during calibration). The MWCLS method is found to be vastly superior to partial least squares (PLS) in this case of limited numbers of calibration samples.

Key Words: Inductively coupled plasma-atomic emission (ICP-AES), Classical least squares (CLS), Multi-window classical least squares (MWCLS), Quantitative elemental spectroscopy, Multivariate analysis

*Sandia is a multi-program laboratory operated by Sandia Corporation, a Lockheed Martin Company, for the United States Department of Energy under Contract DE-ACO4-94AL85000.

INTRODUCTION

Multivariate calibration methods for quantitative spectroscopy are highly developed and have been used in infrared spectroscopy since the early 1980's.[1-5] Early quantitative analyses of inductively coupled plasma/atomic emission spectroscopy (ICP-AES) data could not take advantage of these methods due to the univariate or minimal multivariate nature of the data when single or small numbers of detectors were used. However, with the advent of array detectors, it has become possible to incorporate these multivariate methods into ICP-AES data analysis. Optical emission spectrometers equipped with charge-coupled-device (CCD) detector arrays enable the simultaneous measurement of emission intensities for all wavelengths in the spectral regions of interest.[6-8] Excellent work has already been performed in the area of multivariate analysis of ICP-AES data,[9-15] and van Veen and de Loos-Vollebregt[16] have presented a recent review of the literature related to this subject. However, greater improvements are still possible using multivariate methods previously developed for infrared spectral analysis. To date, the commercial software available with ICP-AES instruments only allows multivariate methods to be applied individually to discrete spectral windows centered near the peak of the emission line for the analyte in a given window.[9-10] This single-window multivariate approach limits the realization of the full power of multivariate data processing methods for the rich atomic emission spectra captured by the array detector. Current ICP-AES multivariate analyses can especially gain in the area of the quantitative determination of trace elements when analyte emissions overlap emissions of elements not included in the calibration. ICP-AES can also take advantage of the classical least squares (CLS) multivariate methods that rely on explicit additive linear spectral models since the emission signals from ICP-AES tend to be additive and linear over a large dynamic range. The application of various single-window CLS multivariate methods to

ICP-AES spectra has already been shown to improve prediction precision and detection limits relative to univariate peak height methods with off-line spectral background correction.[9-10]

One problem encountered with single-window multivariate methods is the question of which window to use when multiple emission lines are present for a given element. The best single window to employ depends on the amount of overlap between all elements in the calibration, the linearity of the emission intensities within a window, the overlap with spectral lines of elements not included in the calibration, and the baseline variation present in the window during analysis. When the emissions within a window experience the above complexities, the analysis results can be quite different between each of the multiple windows used for analysis of each element. Selecting the window yielding the most accurate and precise results for each element in an unknown sample can be quite tedious, time consuming, and expensive. Moreover, the best window can change from sample to sample for a given element.

An alternative to selecting just one window is to let the data automatically define a statistically determined weighted average of the results from all windows such that the final result is optimal.[2] The advantages of this multi-window approach include elimination of tedious operator decisions, decreasing the detrimental effects of spectral overlap with elements not included in the calibration, reduction of problems with nonlinear responses, and generation of a single result for each element that will often have better precision and accuracy than possible from the determination of each element's concentration using spectral data from any single window.

In this paper, we adapt the CLS methods developed for IR spectroscopy[1-3] and apply them to ICP-AES data. A comparison of univariate, single-window CLS methods, and our newly adapted multi-window CLS (MWCLS) method will be presented for several types of samples. It

will be shown that the new methods improve the accuracy, detection limits, and quantitative range. Additionally, the new analysis method decreases the number of dilutions required for complex samples of widely varying levels of analytes. Finally, the new method can even provide for the automatic detection and eventual quantification of elements not included in the original calibration models.

EXPERIMENTAL

Since one of the most challenging tasks facing the analytical atomic spectroscopist is the quantitation of trace elements in material or environmental samples in the presence of major concentrations of interfering elements, we prepared samples to evaluate the ability of various methods to handle these difficult cases. The element concentration ranges of one set of test solutions were defined based on previous assays of electronic scrap that contained small quantities of Resource Conservation and Recovery Act (RCRA) regulated hazardous metals including Pb, Cd, As, Se, Ag, and Cr, and the precious metals Au, Pt, and Pd, in a compositional mix of aluminum, iron, and copper alloys. Accurate determinations of the trace metal concentrations were required to characterize the source materials as being, for example, either hazardous solid waste or recyclable precious metal scrap. Another set of solutions was prepared to represent the "inverse" composition consisting of trace base-metal contaminants in high-purity precious metal alloys.

Test solutions were prepared from National Institute of Standards and Technology (NIST) spectrometric solution standard reference materials (SRM's) or high-purity NIST-traceable stock solutions from commercial suppliers. Dilutions were made gravimetrically using a computer-controlled balance. For those stock solutions certified in volumetric concentration units (μg/mL),

densities were measured in order to convert concentrations to units of μg/g (i.e., parts per million, ppm).

Two sets of calibration standards and a set of validation mixture samples were prepared gravimetrically. One calibration set contained 12 single-element solutions at 100 μg/g. The other calibration set contained four mixed-element standards (Cal-1, Cal-2, Cal-3, and Cal-4). Multi-element validation samples were prepared to simulate samples with compositions of interest in our laboratory. Several of the validation samples contained elements at concentrations greater than present in the calibration samples in order to test the ability of the various models to extrapolate beyond the range of the calibration sample concentrations. Table I presents nominal element concentrations for all samples other than the 100 μg/g single-element calibration set. Actual reference concentrations were determined to four significant figures. The mixed-element calibration set was designed to avoid spectral interferences among elements in the same solution and was used to calibrate the spectrometer using the instrument-supplied calibration software. The single-element calibration sample set was used to build the MWCLS calibration models. Because the instrument software allowed a maximum of only 10 calibration standard entries, the 12 standards in the pure-element calibration set could not be used for calibration when using the instrument software.

During the preparation of the calibration and validation samples, stock solutions of each element in nitric acid were selected wherever possible. However, Au and Pd stock solutions were available only in hydrochloric acid. These elements could not be mixed with Ag in the same solution. Therefore, Sample 1 contains Ag at 0.1 μg/g but does not contain Au or Pd. Sample 2 has a similar composition to Sample 1 but contains Au and Pd at 0.25 μg/g with no Ag. Sample 3 is similar to Sample 2 but contains Pt as an "unknown" element not included in any

calibration sample. Likewise, Sample 4 and Sample 5 are similar in composition except that 4 μg/g Pt has been added to Sample 5. Both Samples 3 and 5 contain Pt as an element that remains unmodeled in all calibration models since Pt was not present in either calibration sample set. A multi-element "control" sample was prepared with all elements (except Ag and Pt) present at 10 μg/g to check the linearity of the calibration curves. A separate control sample with ~10 μg/g Ag was also prepared so that the multi-element and Ag samples together represent the complete 12-element set of calibration elements. Mg was added to each test solution as an internal standard prior to final dilution with 2% HNO_3. The final Mg concentration in each sample was nominally 4 μg/g but the exact concentration was recorded to correct the Mg intensities for small concentration differences in the Mg internal standard. The emission spectra for each sample could then be normalized to the intensity of the concentration-corrected Mg internal standard emissions. Mg was chosen as an internal standard since it has four strong emission bands, two from atomic and two from excited ion states.

All calibration standards and test samples were analyzed using a Perkin Elmer (PE) Optima 3000 ICP-AES equipped with an autosampler. The design and performance characteristics of the Echelle grating optical system and segmented-array CCD (SCD) detector have been described in the literature.[6-8] The instrument operating parameters and sampling times are shown in Table II. The detector arrays used for these analyses are presented in Table III. The segmented pixel arrays (spectral windows) listed in Table III are defined by the wavelength of the major element emission line detected in that window. The SCD detector has 224 windows available, but only data from windows containing the major peaks for the 12 elements used in the calibration and the Mg internal standard were examined. After intensity correction for the Mg

internal standard, a total of 46 windows (3088 pixels) were selected for inclusion in the MWCLS analysis of each element in each sample.

The low-resolution mode of the spectrometer (without scanning) provided a minimum of 14 pixels in each window. However, this number of pixels did not provide enough measurements per window to optimize the MWCLS methods when 12 elements plus baseline components were included. A minimum of 16 spectral intensities is required for our MWCLS analysis; 12 for the elements included in the calibration, 3 for a quadratic baseline, and at least one to determine the spectral residuals necessary for calculating a weighted average of the results from each window. Therefore, the spectrometer was operated in the high-resolution scanning mode so that each window would contain at least 56 pixel measurements. In the scanning mode, a spectrometer mirror is used to move the plasma image in four incremental steps across the detector array, with a pixel intensity reading taken at each step.

The instrument workstation operating system is SCO (Santa Cruz Operation) UNIX, Open Desktop, running Perkin Elmer's Optima 3000 software, version 1.40. The software provides several modes of data collection and processing that can include the application of various background correction methods. One very useful feature of the software is that the raw intensity data can be stored and subsequently reprocessed with different background correction methods. Thus, a direct comparison can be made between alternate spectral correction methods applied to the same data set. In order to compare PE Optima data processing techniques with our multivariate analysis software, it was necessary to develop software to access the raw data files stored by the Optima software in binary format. The interface program reads the PE spectral files and generates a single file of spectra and concentrations compatible with the Sandia National Laboratories' multivariate software package (PLS2000). The Sandia software is written in the

Array Basic language supported by GRAMS from Galactic Industries Corp. Although there were obvious spectral gaps between the array segments selected for these analyses (Table III), the spectra were interpreted as a continuous series of pixels, from low to high wavelength, to avoid display incompatibilities with the multivariate software.

The complete set of calibration standards and test solutions was analyzed in triplicate through the course of one autosampler run. Each set was randomized internally with the exception of the multi-element calibration standards run at the beginning of each set to establish a continuously updated calibration curve for the instrument-supplied software. The subset of multi-element standards was internally randomized so that the run order was different for each of the triplicate analyses. Blank solutions (2% HNO_3) with and without the Mg internal standard were inserted at regular intervals in the run to monitor changes in the spectral baseline.

Analyses with the MWCLS method used sample spectra with the first-run blank subtracted from all subsequent spectra. Relative intensities of the Mg internal standard were based upon shot-noise weighted CLS predictions (see Theory Section). The first sample in the run was used as the calibration standard for the CLS Mg prediction and was assigned a relative Mg intensity of 1.0 for the average of two of the spectral bands of Mg (280.2 nm and 285.2 nm). These two bands were the most representative of the variations of the majority of emissions from the 12 elements used as analytes. Simultaneous linear baseline fits were included in the CLS determinations of the relative Mg intensities for all other sample emission spectra. These relative intensities were also corrected for the actual concentrations of the internal Mg reference in each sample. During subsequent CLS analyses for the 12 analytes, each sample spectrum was divided by the concentration-corrected relative Mg intensity to correct for intensity fluctuations between sample spectra.

After the spectra were collected, it was discovered that many were contaminated by carryover of some of the elements from previous samples. This carryover problem was later found to be a result of the specific ICP spectrometer operating conditions used. The carryover complicated the analysis of the spectra and may have limited the calibration results from the PE-Optima multivariate spectral analysis method.

THEORY

Univariate Analysis

Emission intensities were measured for standards and samples in each window using the Optima software. The emission line peak location for each window is determined by the Optima software using a parabolic fit of the most intense pixel reading and the two adjacent points. The emission intensity measured at the peak pixel corrected for the background intensity is then used for calibration and analysis. The auto-background correction feature of the software was used to correct for baseline shifts due to spectral overlaps. This feature utilizes an off-line background correction technique that employs a search algorithm to find the baseline intensity for a given spectral window by measuring the slope of the emission background away from the peak. The "baseline" intensity is then subtracted from the peak intensity, and the resulting net intensity is ratioed to the concentration-normalized internal standard (Mg) emission intensity. A two point, linear regression calibration was established for each element for each of the segmented arrays listed for that element in Table III using the 100 µg/g standard for that element and the 2% HNO_3 blank solution with the Mg internal standard present. The instrument-supplied univariate calibration methods were used directly for the univariate methods presented in this paper.

Multi-Component Spectral Fitting (MSF)

The "Multi-component Spectral Fitting" (MSF) is an Optima 3000-supplied multivariate CLS method that models the sample spectrum as a linear combination of pure-element spectral profiles in each spectral window.[9-10] MSF operates independently within each spectral window (array segment) so that a separate model is constructed for each window. The models are constructed in advance of the analysis with pure-component solutions each at 100 µg/g, and the models presume that all components in the "unknown" sample are known. Baselines are incorporated in the model by including the baseline from the blank in the CLS fitting procedure. The PE-Optima MSF software uses the 4 multi-element calibration standards (see Table I) to update earlier MSF calibration models during the experimental acquisition of all the sample spectra. Again, the Mg internal standard emission intensities were used to normalize intensities for instrument variations.

Multi-window CLS Method

The basic MWCLS method has been presented previously for IR spectral analyses.[1-3] A detailed mathematical description of the algorithms, as specifically adapted for ICP-AES analyses, is included in the Appendix. The algorithm assumes a linear additive model for each spectral window. During CLS calibration, least-squares estimates of each element's spectrum in each window were obtained using the 36 pure-element calibration standards spectra (12 pure-element samples at ~100 µg/g run in triplicate). These estimated pure-element spectra have higher signal-to-noise ratios than an individual pure-element sample spectrum since they are derived from multiple calibration spectra. In practice, CLS calibration models could be derived from mixture solutions of elements to be calibrated. This calibration requires that the number of independent calibration standards equals or exceeds the number of elements modeled.

During the CLS prediction phase, all pure-element spectra from the calibration plus a choice of polynomial baselines up to third order are simultaneously used in a CLS prediction step for each spectral window. For the prediction results presented here, a quadratic baseline was selected and simultaneously included in the CLS prediction with the 12 pure-element spectra estimated during the CLS calibration. In addition, we performed a weighted least squares prediction that assumes the spectral noise is shot noise limited (i.e., the noise increases as the square root of the signal). The weighting primarily affects the concentration estimates of elements with the largest emission intensities.

CLS prediction is performed separately for each spectral window, which allows for a different quadratic baseline to be fit for each spectral window of each sample spectrum. The result is a series of 46 determinations (one for each window used in the analysis) for each element in each sample. The final concentrations reported for a given sample are based upon a weighted average of the 46 concentrations for each element obtained from the 46 windows. An element's weight for a given window is proportional to the reciprocal of the product of the diagonal term for that element in the inverse covariance matrix and the residual spectral variance for the window (see the Appendix for details). In other words, the weights used in the weighted average concentration for each sample are based upon the inverse of the signal-to-weighted-noise variance for each element in each window. The weighted-noise variance is proportional to the sum of squared spectral residuals for the weighted CLS fit for each window and, therefore, this noise variance term is the same for all elements in a given window. The signal variance is derived from the inverse of the covariance matrix and is effectively the square of the net-analyte signal[17] (i.e., the portion of the analyte signal orthogonal to all other calibration element signals that may be present in the spectral window) for each element. The net-analyte signal differs for

each element in each window and is a function of both the strength of the element's signal and the degree of overlap with interfering elements. More intense element signals tend to yield larger weights. However, greater overlap of emissions in a given window reduces an element's net-analyte signal, causing a reduction in the weight used in the weighted average concentration for the element in that window. If spectral residuals are large in a given window due to 1) the presence of unmodeled elements, 2) nonlinear responses, 3) spectrometer drift, or 4) inadequate modeling of the baseline, then the weighting for all elements in that window will be reduced relative to a window where the spectral residuals are small.

The weighting by the inverse variance of the signal-to-weighted-noise results in weights that vary over 16 orders of magnitude for the 46 windows and samples considered here. Thus, the weighted average serves the purpose of efficiently minimizing the influence of windows with either little or no net analyte signal or large spectral residuals due to model inadequacy. The use of the weighted average eliminates the need for operator selection of the windows. A single result is reported that represents a statistically efficient summary of the results from all windows included in the analysis.

Because carryover of some elements from one sample to the next was a problem, special methods were required to minimize the effect of carryover in the pure-element spectra estimated during CLS calibration. The carryover was observed to be present with six of the 12 elements used in the calibration and caused elements experiencing carryover to be present in all calibration samples, in all validation mixture samples, and in all blank samples except the first blank sample. The presence of these carryover elements in all samples caused the carryover element spectra to be present at low levels in the CLS-estimated pure-element spectra. Therefore, after our initial MWCLS calibration, the amount of each carryover element in each estimated pure-element

spectra was determined by a separate CLS determination of the carryover element's concentration in each of the 12 CLS-estimated spectra. The carryover element concentrations were determined using only the primary windows for the carryover element and those spectral regions within the windows that were not visually contaminated by overlap with the other 11 elements. This concentration-correction procedure was performed one element at a time.

New CLS estimates of the pure-element spectra were then generated after the concentration of a given carryover element was determined in all 12 of the CLS-estimated pure-element spectra. A second CLS calibration was then performed using the original CLS-estimated pure-element spectra and a calibration concentration matrix that included the new CLS-estimated concentrations of the carryover element. The CLS-estimated pure-element spectra obtained from this second CLS calibration contained no visual contamination of any of the 12 estimated pure-element spectra by the selected carryover element. This procedure was repeated for the other five elements experiencing carryover problems. The final iteration resulted in CLS-estimated pure-element spectra exhibiting no carryover contamination above the spectral noise level. These corrected pure-element spectra were used in the MWCLS predictions of all validation and blank samples. Because of the presence of the carryover problem, all sample spectra must be considered contaminated to some small degree by one or more of the six elements experiencing carryover. Therefore, the computation of detection limits and the determination of low concentrations with real samples are restricted to the six elements not experiencing carryover (i.e., Al, As, Cr, Ni, Pb, and Pd).

RESULTS AND DISCUSSION

Figure 1 presents the superimposed emission spectra of all calibration and validation samples. The spectra cover the region from 167 to 420 nm but are presented by pixel number rather than wavelength since there are both gaps and overlaps between the 46 spectral windows.

Figure 2 demonstrates the carryover problem with Cu, which exhibited the greatest degree of carryover of the 12 elements investigated. Repeat samplings of a 100 μg/g Cu solution, interspersed with 6 consecutive samplings of a 2% HNO_3 blank solution, demonstrated that the carryover can be as much as 0.2 μg/g Cu over the approximately 10 min. interval between Cu samplings. Figure 2 clearly demonstrates the magnitude of the problem when the ICP auxiliary flow rate of 0.5 liter/min Ar was used and suggests that the contamination can extend over multiple samples since the time spacing between samples was similar to that used in the study. It was later determined that carryover could be eliminated by operating the ICP at an auxiliary Ar flow rate higher than the default setting of 0.5 L/min used for the study. Figure 2 also shows the results of a second analysis of the same sample set obtained using an ICP auxiliary flow of 1.0 liter/min Ar. The Cu signal-to-noise ratio was essentially the same in both cases with no loss in sensitivity at the higher flow setting. Because an internal Mg standard was not run in these Cu carryover tests, correction for system drift was not possible, and a slight drift of the baseline intensities was observed in Fig. 2 for both flow rates. Since a higher auxiliary flow will "lift" the plasma off the sample injector tip in the ICP torch configuration, it may be that the "carryover" observed with the lower flow setting is the result of deposition and release of atomized copper on the injector tip from the 100ug/g Cu sample.

The power of the MWCLS method is demonstrated by the following discussion using a simplified three-window As analysis. Arsenic is selected because one of its windows contains an emission from the unmodeled Pt element and another As window is almost completely overlaped

with a Pd emission line. Fig. 3A shows all 12 of the pure-element emission spectra (each at ~ 100 μg/g) in the three As windows. The unmodeled Pt emission is not shown since its emission spectrum was not present in any calibration spectrum. Fig. 3B shows the same 12 emission spectra scale expanded in the intensity axis so the degree of spectral overlap can be seen more clearly. There is nearly direct overlap of As and Pd emissions in the first As window. The MWCLS algorithm generates separate As concentrations for each of the three windows in Fig. 3. The final As concentration is determined by a weighted average of the three As concentrations as described in the Appendix. When As is the only element in the calibration and prediction samples, then the relative weights for the pure As element sample are 35%, 31%, and 34% for the 189.0 nm, 193.7 nm, and 197.2 nm bands of As, respectively. These weights are dominated by the relative signal strengths of the three As bands rather than the magnitude of the spectral residuals since the sum of squared spectral residuals are similar in magnitude for each window. However, if the other 11 elements are included in the calibration model along with As, the weights for analysis of a single-element As sample become 4%, 42%, and 54% for the same three windows, respectively. The first band has greatly diminished influence because of the As and Pd overlap at 189.0 nm. Thus, the net-analyte signal for As is reduced for this window, and the result from the first window is given relatively low weight during prediction of As in samples.

Fig. 4A shows the three As spectral windows for a validation sample containing As at 1.00 μg/g. This sample contained 11 of the 12 elements included in the MWCLS calibration model. In addition, it contained a Pt impurity at 4 μg/g that was not included in the calibration (Sample 5 in Table I). Fig. 4B shows the individual spectral residuals using a 12 element CLS model (without Pt) applied to each As window for this multi-element sample with unmodeled Pt present in the second As window. The CLS As determinations from the individual windows for

this sample are 1.02 μg/g, 1.13 μg/g, and 1.01 μg/g, for the 189.0 nm, 193.7 nm, and 197.2 nm As bands, respectively. Therefore, a simple average of the results from all windows (i.e., 1.05 μg/g) would degrade the accuracy of the As predictions. Due to the large spectral residuals in the second window, the weights for this band are greatly reduced in the As determination. The weighting is now 10.5%, 0.5%, and 89% for the three windows, respectively. Thus, the CLS prediction of this sample is nearly unaffected by the presence of an unmodeled Pt emission, and the weighted average predicted As concentration is 1.01 μg/g while the reference As concentration is 1.00 μg/g. For accurate predictions, at least one of the As windows must follow the linear additive CLS model. The weighted average As result was automatically defined by the CLS calibration model and the characteristics of the sample spectrum. The final prediction result required no decisions or input by the analyst, a significant advantage for the rapid ICP-AES analysis of complex multi-element samples.

Figure 4C demonstrates another advantage of the MWCLS method. If we examine the CLS spectral residuals for each window in Fig. 4B, we observe that window 2 has experienced a problem that was not encountered in either window 1 or window 3. The problem with window 2 could be the presence of emission from an element not included in the calibration or the problem might be due to nonlinearity in the spectrum of this sample. Unfortunately, the spectral residuals in Fig. 4B do not indicate the source of the large residuals in the second window since the least squares fit using 12 elements in the model for each window causes the spectral residuals to become more random. However, the MWCLS approach allows an alternate method of reconstructing the measured spectrum to yield a more informative residual spectrum. The CLS calibration generates precise estimates of the pure-element emission spectra. The MWCLS prediction yields more accurate element concentrations. Therefore, reconstructing the measured

spectrum can be performed by multiplying the estimated pure-element spectra by their MWCLS estimated concentrations and summing the contributions from all elements in the model. Since the weighted-average prediction results are generally unaffected by unmodeled interfering emissions, the resulting residual spectrum obtained by subtracting this new reconstructed spectrum from the measured spectrum should simply represent any unmodeled emissions and spectral noise. The spectral residuals resulting from this latter calculation are presented in Fig. 4C. Note that the resulting residual spectrum is now quite different and indicates clearly the presence of an uncalibrated impurity emission located at 193.7 nm. Checking the elements having an emission at this wavelength allows us to detect and identify a Pt impurity in the sample. Once we have identified the impurity element, we could quantify its concentration by running a calibration standard for the uncalibrated Pt element. Thus, significant interpretation advantages flow from the MWCLS analysis.

Fig. 5 shows the MWCLS prediction ability for Al at concentrations ranging from 0 to 300 μg/g in samples that contain as many as 11 other elements at a variety of levels from 0 to 150 μg/g. The overall standard error of prediction (SEP) for Al concentration for these samples is limited by source fluctuations for the high concentration samples rather than by spectral signal-to-noise ratios. Thus, the higher precision potential of the MWCLS procedure is not generally realized with high concentration analytes even when all elements are known and included in the analysis. However, the MWCLS procedure can yield a dramatic improvement in the ability to accurately determine trace elements in the presence of interferences.

The improvement in low-level determinations is even more dramatic when one or more interfering elements in the samples are not included in the calibration. The improvement using the MWCLS analysis is readily demonstrated in Table IV. Table IV shows the PE-Optima

univariate, PE-Optima MSF, and the MWCLS methods applied to the same selected validation sample spectra. The results are shown for the determination of the minor elements in the selected multi-element samples and are presented as the average value for the triplicate analyses and the standard error of the mean for the three replicate measurements. The replicates span 10 to 16 hr of elapsed time and, therefore, include the effects of spectrometer drift over this time period. In general, the predicted concentrations for the major elements were close to the known values and are not shown. The two PE-Optima models perform reasonably well for some element windows shown in Table IV. Surprisingly, the univariate method does almost as well as the MSF model in some cases, indicating that some of the overlaps are most likely sloping backgrounds and not direct emission overlaps. For the predictions of the elements shown in Table IV, neither PE model performs well in all wavelength windows, and it is not apparent which array yields the correct result without prior knowledge of the element concentration.

The ease of analysis and improved accuracy of the MWCLS method are demonstrated for a few samples with trace elements present as shown in Table IV for Ag, Pb, and Pd. First, only a single weighted-average result is reported for each element based upon all 46 windows used in the analysis. The MWCLS prediction results when all 12 elements are included in the CLS calibration model (MWCLS-12) are always more accurate than the average of the PE-Optima univariate or MSF predictions and more accurate than the individual window results in every case except for As in Sample 4. In addition, Table IV presents MWCLS results that represent models with only a single element in the model (MWCLS-1). Even though the other 11 elements are not included in the model, the MWCLS-1 approach is only slightly degraded by the absence of the other elements in the CLS models. In fact, none of the MWCLS-1 predictions in Table IV are degraded to the level of the MSF models that include all 12 elements in the calibration

models. The ability of the MWCLS-1 models to perform accurate predictions in the presence of multiple unmodeled elements derives from the simultaneous use of all 46 spectral windows with the final prediction result reported as the weighted average concentration of all windows. As mentioned previously, accurate results are expected if just one of the windows containing the analyte element emission is free of interference or if any unmodeled emission can be adequately fit by the separate quadratic baseline included in the CLS analysis of each spectral window.

The MSF models should work better than is evidenced here. The models were developed in advance of the sample analyses, and it is possible that some wavelength drift or other source of spectrometer drift occurred during that interval. Calibration samples were run during the study to update the MSF model, but the updating may not correct for all sources of system drift. It is likely that with the knowledge gained from these initial PE analyses, "proper" wavelength selection, and further refinements of the MSF pure-component models, we could eventually develop more accurate MSF results for these materials. This is how spectroscopists have historically done method development. The new MWCLS method circumvents this tedious, time-consuming process and directly yields accurate results without analyst intervention.

Table V presents the average predictions of all single and multi-element samples whenever the listed target element was not present in the sample. Table V shows only results from those six elements experiencing no carryover. This table represents the ability of the various models to detect the absence of elements when one or more other elements are present in the samples. The closer the numbers are to 0 ng/g in Table V, the better a given model has succeeded in eliminating the detrimental effects of spectrally interfering elements in the samples. Table V not only includes the PE-Optima univariate, PE-Optima MSF, and 12-element multi-window CLS results (MWCLS-12), but it also includes the MWCLS-1 case where only the target

element has been included in the calibration model. This latter case represents a very severe and extreme case where the CLS model does not include the effects of overlapping spectral interferences. Both univariate and MSF methods report the results individually for each window, demonstrating that prior knowledge of the analyte concentration or presence of interfering elements must be known to properly select the best window to report results. Even if the best window can be selected with the univariate and MSF methods, it is observed in Table V that the MWCLS-12 method almost always outperforms even the best single-window predictions using either the PE univariate of MSF methods. The MWCLS-12 method always provides lower standard deviations for repeat predictions. In addition, the degradation in accuracy is not very great for the MWCLS-1 method that includes only the target element in the calibration model. In fact, only for As does the MSCLS-1 model underperform the precision of the PE MSF method for the best window, and in this case, the relative difference in prediction is not statistically significant. These results clearly demonstrate the power of the MWCLS method to mitigate the detrimental effects of unmodeled interferences in the sample spectra.

The analyses of our data give the opportunity to estimate detection limits for each element in the presence of modeled and unmodeled interferences. Usually the method for calculating detection limits is based upon analysis of blank solutions without interferences present.[18-20] These standard methods of determining detection limits are not used here since they are overly optimistic for the analysis of real samples with interferences. If we obtain the standard deviations of each element for all samples with the element absent but with one or more ineterferences present, then we can estimate detection limits for our real samples in order to compare the detection performance of each analysis method. Table VI presents the average 3σ detection limits for the six elements not experiencing carryover using the same models and

sample analyses presented in Table V. Here the range of detection limits given for the single-window methods represents the analyte windows yielding the best and worst detection limits using the set of windows normally used for each target element determination. These detection limits are the detection limits expected for these real samples with interfering elements present in the samples. Obviously, these reported detection limits depend on specifics of the actual samples, that is the intensity and numbers of overlapping emission bands. The results in Table VI only demonstrate detection limits expected for the elements and samples included in this study. Nevertheless, the results clearly demonstrate the superiority of the MWCLS method even when all interfering elements are left out of the calibration model. The measured 3σ detection limits in Table VI demonstrate that the MWCLS-12 method always outperforms the univariate and MSF methods. In fact, in the worst case example using the poorest window for Pb, the MWCLS-12 model outperforms the MSF method by a factor of nearly 200. Only in the case of As does the best window MSF model slightly beat the detection limit of the MWCLS-1 method that includes only the single target element in the calibration model. The MWCLS-1 prediction algorithm applied to As cannot recognize problems with the presence of Pd interference since the direct overlap between As and Pd emissions in the 189.0 nm window does not cause an inflation of spectral residuals when both As and Pd are present. Therefore, CLS cannot detect a problem with this window if Pd is present in the sample but not included in the calibration model.

Finally, since partial least squares (PLS) methods generally outperform traditional CLS methods, we applied standard PLS methods to these same data. In both CLS and PLS calibrations, only the 36 single element 100 μg/g samples spectra were included in the calibration (12 samples repeated in triplicate within a 16 hr period). PLS analyses were applied to all 46 windows and also applied only to those windows normally used for quantifying the target

element. For the PLS analysis applied to all 46 windows, PLS sometimes performed extremely poorly even for high concentration elements (e.g., As, Pb, and Se) resulting in essentially no predictive ability. For the other elements, the PLS predictions were generally good when their concentrations were high, but were very poor for all elements when they were present at low concentrations. PLS calibrations based upon only the target element windows showed improvement over the 46 window PLS calibrations, but still the PLS prediction results did not compare favorably to the MWCLS predictions for the minor components. The poor performance of PLS was due to a combination of factors including the calibration design, the small number of calibration samples, the difficulty in PLS modeling the baseline drift over large spectral ranges, and the inability of the PLS model to handle the carryover problem.

CONCLUSIONS

We have demonstrated that the MWCLS method applied to ICP-AES spectral data has significant quantitative and qualitative advantages over standard univariate and single-window CLS (i.e., PE-Optima MSF) analysis methods. The MWCLS method even significantly outperforms standard PLS methods. In the best case, the newly applied MWCLS method improves detection limits by more than 2 orders of magnitude relative to the commercial MSF method. Accuracy, precision, and detection limits have all been demonstrated to be better with the MWCLS method. The new method has also been demonstrated to be relatively immune to unmodeled interferences. Thus, the requirement that all interfering elements be included in the CLS calibration is removed. In addition, the analyst is freed from the tedious and time-consuming task of deciding which target element windows to select when each window yields different analytical results. It is also evident that the new MWCLS methods can reduce the need

for running preliminary survey analyses of unknown samples followed by either the pretreatment of the samples to eliminate interfering elements or the generation of better matched calibration samples. Although not shown in this paper, it is expected that when sample concentrations become very large, then nonlinear self-absorption effects will degrade the linear behavior of the stronger emission lines. The MWCLS methods described here will eliminate the need for analysis of serially diluted samples to cover the range of both major and minor species. The latter result is expected since the saturation of an emission line will change its shape and cause the spectral residuals to be relatively large for any saturated bands. Therefore, the MWCLS weighted average result will automatically shift emphasis in the weighted average to the more linear lower intensity bands. This shifting of analysis emphasis to the more linear bands has been demonstrated to improve accuracy for MWCLS analysis of IR spectra at high concentrations of N_2O in air.[21]

The results presented in this paper lead us to speculate that, in the future, calibrations generated for all 70 of the elements measured with ICP-AES could be included in a global instrument model to achieve at least semi-quantitative results without the need to run any standards. Since multivariate methods are known to be very sensitive to instrument drift and instrument differences, studies to evaluate the reasonableness of the above speculation are needed and are currently underway in our laboratory.

ACKNOWLEDGEMENTS

The authors acknowledge Edward V. Thomas for calibration designs and Howland D. T. Jones for aiding in the preparation of all the samples used in this study.

APPENDIX. Weighted MWCLS Algorithm

For this discussion, bold upper-case letters represent matrices, vectors are given lower-case bold letters, and scalars are indicated by lower-case letters in italics. We use the convention that all vectors are written as column vectors so row vectors are expressed as transposed column vectors. The linear additive classical least squares model can then be written as

$$\mathbf{Y} = \mathbf{BX} + \mathbf{E} \qquad (1)$$

where $\mathbf{Y}$ is the $n \times p$ matrix of p spectral intensities of the n samples in the calibration set, $\mathbf{X}$ is the $m \times p$ matrix of p spectral intensities representing the m pure-component spectra at unit concentration, B is the $n \times m$ matrix of concentrations of the n samples for each of the m spectral components, and $\mathbf{E}$ is the $n \times p$ matrix of spectral errors representing spectral noise and possibly model error. Generally in statistical models, the B matrix represents the estimated coefficients while the $\mathbf{X}$ matrix represents the independent variables. However, during CLS calibration and prediction, the parameter being estimated in Eq. 1 changes. Rather than changing notation between CLS calibration and prediction to remain consistent with the standard statistical notation, we chose to keep the notation constant. Since our first description of the multi-window CLS approach dealt only with prediction, we maintain the notation used in the Appendix of Ref. 2 based upon CLS prediction. Therefore, during CLS calibration the matrix X is estimated and the B matrix represents the independent variables. During prediction, B is estimated and X represents the independent variables.

During classical least squares calibration, we solve for the least squares estimated pure-component spectral matrix $\mathbf{X}$. The least squares solution to Eq. 1 is

$$\hat{\mathbf{X}} = (\mathbf{B}^T\mathbf{B})^{-1}\mathbf{B}^T\mathbf{Y} \qquad (2)$$

The $\mathbf{Y}$ matrix can be centered first (i.e., the column mean of $\mathbf{Y}$ is removed from each row of $\mathbf{Y}$) to improve computational precision and to remove a spectral intercept at each wavelength. Alternatively, an intercept term can be fit at each wavelength by adding a column of ones to the B matrix. The dimensions of $\hat{\mathbf{X}}$ will then be $(m+1) \times p$. If the spectra are first corrected for an internal reference, then the column of ones in the B matrix should be replaced by the inverse of the scaling parameter obtained from the internal reference peak.

It is assumed that $\mathbf{E}$ is a noise matrix that is a random observation from a probability distribution that has a mean of zero and a variance of $\sigma^2\mathbf{V}$, where $\mathbf{V}$ is a known $p \times p$ matrix and σ^2 can be estimated from the spectral residuals. Then the weighted least squares estimate of $\mathbf{X}$ can be obtained one wavelength at a time as described in Reference 3. Once the least-squares estimate of $\mathbf{X}$ is obtained from the calibration, then this $\hat{\mathbf{X}}$ matrix can be used for concentration prediction of a sample spectrum $\mathbf{y}$ (vector of dimension $1 \times p$). The $\hat{\mathbf{X}}$ matrix can also be augmented by a row of ones to account for spectral offsets, a row of evenly incremented integers for linear baselines, and a row of squared integers for quadratic baseline corrections to the model. The latter two rows should be mapped from -1 to 1 to provide better computational precision. The model for predicting sample concentrations from the unknown sample spectrum, $\mathbf{y}$, is then

$$\mathbf{y} = \hat{\mathbf{X}}^T\boldsymbol{\beta} + \mathbf{e}. \qquad (3)$$

Note that the convention of presenting vectors as column vectors reverses the order of Eq. 3 relative to that of Eq. 1. The weighted least squares estimate of the sample concentrations, $\hat{\boldsymbol{\beta}}$, is

$$\hat{\boldsymbol{\beta}} = (\hat{\mathbf{X}}\mathbf{V}^{-1}\hat{\mathbf{X}}^T)^{-1}(\hat{\mathbf{X}}\mathbf{V}^{-1}\mathbf{y}) \qquad (4)$$

The m × m covariance matrix of $\hat{\boldsymbol{\beta}}$ is

$$\mathbf{C}(\hat{\boldsymbol{\beta}}) = \sigma^2(\hat{\mathbf{X}}\mathbf{V}^{-1}\hat{\mathbf{X}}^{\mathrm{T}})^{-1} \qquad (5)$$

and the unknown σ^2 is estimated by

$$\hat{\sigma}^2 = \frac{(\mathbf{y}^{\mathrm{T}}\mathbf{V}^{-1}\mathbf{y}) - \hat{\boldsymbol{\beta}}^{\mathrm{T}}(\hat{\mathbf{X}}\mathbf{V}^{-1}\mathbf{y})}{p-m} \qquad (6)$$

We assume here that the errors are independent but with different variances at each wavelength for each spectrum. In the case of independent errors, **V** is diagonal and can be easily inverted by inverting its diagonal elements. For shot-noise limited detectors encountered in our ICP-AES data, the diagonal elements of **V** can be estimated for each sample spectrum **y** by using the elements y_i at each wavelength i as the diagonal elements of **V** since the variance of the shot noise increases directly with the spectral intensity.

The above CLS prediction can be performed separately for each spectral window. The result is a series of w concentrations, one for each component in each of the w windows. The final calculated concentrations for each analyte can be formed by a weighted average of the concentrations found for each analyte in each window. The least-squares estimated concentration for component j in the k^{th} window is $\hat{\boldsymbol{\beta}}_{kj}$. The matrix $(\hat{\mathbf{X}}^{\mathrm{T}}\mathbf{V}^{-1}\hat{\mathbf{X}})_k^{-1}$ is used to estimate the variance of $\hat{\boldsymbol{\beta}}_{kj}$. Let s_k^{jj} be the j^{th} diagonal element of $(\mathbf{X}^{\mathrm{T}}\mathbf{V}^{-1}\mathbf{X})_k^{-1}$ corresponding to $\hat{\boldsymbol{\beta}}_{kj}$. The s_k^{jj} diagonal element represents the inverse of the summary squared net-analyte signal for component j in the k^{th} window. An estimate of σ^2 for window k, i.e., $\hat{\sigma}_k^2$, can be calculated using Eq. 6. $\hat{\sigma}_k^2$ represents a summary statistic proportional to the squared spectral residuals in window k for the sample spectrum. The method to estimate the relative concentration of component j in the mixture is to take a weighted average of the $\hat{\boldsymbol{\beta}}_{kj}$'s where the

weight is the reciprocal of the product of s_k^{jj} and $\hat{\sigma}_k^2$. The reported summary concentration for component j from all windows is given by

$$\hat{\beta}_j = \frac{\sum_{k=1}^{w} (\hat{\beta}_{wj} / (s_k^{jj} * \hat{\sigma}_k^2))}{\sum_{k=1}^{w} (1/(s_k^{jj} * \hat{\sigma}_k^2)} \qquad (7)$$

Eq. 7 gives highest weight to those windows where component j has its largest net-analyte signals and that also exhibit small spectral residuals (i.e., those windows that follow the linear additive model and include in the calibration model all components with intensity in the window). Thus, this weighted average concentration is a statistically efficient measure of the j^{th} component concentration in the sample.

REFERENCES

1. D. M. Haaland and R. G. Easterling, Appl. Spectrosc. **34**, 539-548 (1980).
2. D. M. Haaland and R. G. Easterling, Appl. Spectrosc. **36**, 665-673 (1982).
3. D. M. Haaland, R. G. Easterling, and D. A. Vopicka, App. Spectrosc. **39**, 73-84 (1985).
4. W. Lindberg, J.-A. Persson, and S. Wold, Anal. Chem. **55**, 643-648 (1983).
5. P. M. Fredericks, J. B. Lee, P. R. Osborn, and D. A. Swinkels, App. Spectrosc. **39**, 303-310 (1985).
6. T. W. Barnard, M. I Crockett, J. C. Ivaldi, and P. L. Lundberg, Anal. Chem. **65**, 1225-1230, (1993).
7. T. W. Barnard, M. I Crockett, J. C. Ivaldi, P. L. Lundberg, D. A. Yates, P. A. Levine, and D. J. Sauer, Anal. Chem. **65**, 1231-1239 (1993).
8. J. C. Ivaldi, D. Tracy, T. W. Barnard, and W. Slavin, Spectrochim. Acta, **47B**, 1361-1371 (1992).
9. J. C. Ivaldi and T. W. Barnard, Spectrochim. Acta, **48B**, 1265-1273 (1993).
10. J.-M. Mermet and J. C. Ivaldi, J. Anal. Atomic Spectrometry, **8**, 795-801 (1993).
11. E. H. van Veen, Spectroscopy **7** (6), 39-43 (1992).
12. E. H. van Veen and M. T. C. de Loos Vollebregt, Spectrochim. Acta **52B**, 321-337 (1997).
13. M. F. Pimentel, B. D. Neto, M. C. U. Dearaujo, and C. Pasquini, Spectrochim. Acta **52B**, 2151-2161 (1997).
14. X. H. Yang, J. F. Wei, H. T. Liu, B. Y. Tang, and Z. X. Zhang, Spectrochim. Acta

53B, 1405-1412 (1998).

15. J. Nolte, Atomic Spectrosc. **20**, 103-107 (1999).

16. E. H. van Veen and M. T. C. de Loos Vollebregt, Spectrochim. Acta **53B**, 639-669 (1998).

17. A. Lorber, Anal. Chem. **58**, 1167-1172 (1986).

18. P. W. J. M. Boumans, J. C. Ivaldi, and W. Slavin, Spectrochim. Acta, **46B**, 431-445 (1991).

19. P. W. J. M. Boumans, Spectrochim. Acta, **46B**, 917-939 (1991).

20. P. W. J. M. Boumans, Anal. Chem. **66**, 459A-467A (1994).

21. D. M. Haaland, "Methods to Include Beer's Law Nonlinearities in Quantitative Spectral Analysis," in ASTM Special Technical Publication, Computerized Quantitative Infrared Analysis, G. L. McClure, Editor, STP **934**, 78 (1987).

Table I. Nominal concentrations of elements in solutions

	Cal-1	Cal-2	Cal-3	Cal-4	Sample 1	Sample 2	Sample 3	Sample 4	Sample 5	Control 1	Control 2
	(µg/g)	(µg/g)	(µg/g)	(µg/g)	(µg/g)	(µg/g)	(µg/g)	(µg/g)	(µg/g)	(µg/g)	(µg/g)
Ag	100	0	0	0	0.1	0	0	0	0	0	10
Al	100	0	0	0	300	300	300	1	1	10	0
As	0	100	0	0	1	1	1	1	1	10	0
Au	0	100	0	0	0	0.25	0.25	30	30	10	0
Cd	100	0	0	0	1	1	1	1	1	10	0
Cr	0	0	100	0	20	20	20	1	1	10	0
Cu	0	0	100	0	100	100	100	1	1	10	0
Fe	0	0	0	100	150	150	150	1	1	10	0
Ni	0	100	0	0	50	50	50	35	35	10	0
Pb	100	0	0	0	1	1	1	1	1	10	0
Pd	0	0	100	0	0	0.25	0.25	34	30	10	0
Pt[a]	0	0	0	0	0	0	0.25	0	4	0	0
Se	0	100	0	0	1	1	1	1	1	10	0
Mg[b]	4	4	4	4	4	4	4	4	4	4	4

a. Unmodeled element
b. Internal Standard

Table II. Optima 3000 ICP-AES instrument operating parameters used

RF Power:	1140 W	Sample pump rate:	1.0 mL/min.
Plasma gas:	15 L/min.	Rinse time:	2 minutes
Nebulizer gas:	0.84 L/min.	Read delay:	1 minute
Auxiliary gas:	0.50 L/min.		
Resolution:	normal (62µm slitwidth)		
Radial view			
Scanning:	on		
Integration:	auto (1-10 seconds)		
Replicates:	3		

Table III. Optima 3000 ICP-AES instrument SCD subarrays used

Element	Wavelength (nm)	Subarray number	Element	Wavelength (nm)	Subarray number
Ag	243.8	64	Cu	324.8	153
	328.1	147		327.4	145
	338.3	164	Fe	234.3	68
Al	167.0	6		238.2	93
	237.3	73		239.6	70
	308.2	141		259.9	87
	309.3	131		274.0	110
	394.4	232	Mg	279.1	101
	396.2	236		279.6	103
As	189.0	12		280.3	105
	193.7	8		285.2	115
	197.2	10	Ni	221.6	45
Au	208.2	26		231.6	52
	242.8	85		232.0	71
	267.6	111		341.5	173
Cd	214.4	40	Pb	217.0	42
	226.5	36		220.4	54
	228.8	63		261.4	81
	361.1	195		283.3	120
Cr	205.6	20	Pd	248.9	92
	206.1	24		324.3	152
	267.7	98		340.5	171
	357.9	205		363.5	203
Cu	221.5	43	Se	196.0	15
	224.7	53		204.0	23

Table IV. Prediction results from selected samples using four different calibration methods

Element (Sample ID)	Reference Conc.	Window	PE-Optima Univariate		PE-Optima MSF		MWCLS (12 elements in calibration)		MWCLS (Single element in calibration)	
	(µg/g)		Average (µg/g)	Std. Error of Mean (µg/g)	Average (µg/g)	Std. Error of Mean (µg/g)	Average (µg/g)	Std. Error of Mean (µg/g)	Average (µg/g)	Std. Error of Mean (µg/g)
Ag Sample 1	0.098	Ag243 Ag328 Ag338	88.99 0.090 0.487	0.71 0.001 0.004	-11.426 0.104 0.127	0.29 0.000 0.001	0.100	0.0005	0.091	0.001
As Sample 1	0.998	As188 As193 As197	1.023 0.959 0.984	0.001 0.014 0.008	1.018 1.031 1.060	0.019 0.007 0.009	1.017	0.009	1.017	0.006
As Sample 4	0.999	As188 As193 As197	1.913 1.007 1.012	0.008 0.010 0.007	1.621 1.024 1.003	0.011 0.005 0.006	1.022	0.005	1.121	0.007
Pb Sample 2	1.001	Pb216 Pb220 Pb261 Pb283	1.406 0.994 -2.38 1.323	0.009 0.002 0.70 0.016	0.658 1.021 -3.20 1.080	0.015 0.008 1.3 0.022	1.002	0.004	1.038	0.004
Pd Sample 2	0.247	Pd248 Pd324 Pd340 Pd363	2.82 0.192 0.159 0.272	0.038 0.006 0.002 0.30	0.013 0.275 0.219 0.473	0.038 0.004 0.008 0.008	0.222	0.004	0.260	0.012

Table V. Average prediction of element concentration in samples with no element present

Window	Samples	Reference Value (ng/g)	PE-Optima Univariate		PE-Optima MSF*		MWCLS-12 (12 Element Calibration)		MWCLS-1 (1 Element Calibration)	
			Average (ng/g)	Std. Error of Mean (ng/g)	Average (ng/g)	Std. Error of Mean (ng/g)	Average (ng/g)	Std. Error of Mean (ng/g)	Average (ng/g)	Std. Error of Mean (ng/g)
Al 1670	all with zero Al	0.000	12	12	28	15	0.09	0.3	3	0.3
Al 2373			4	3	-126	65				
Al 3082			7	2	4	0.9				
Al 3092			22	6	-4	3				
Al 3944			16	5	15	5				
Al 3961			-1	2	0	0.9				
As 1889	all with zero As	0.000	279	144	158	95	0.03	0.8	5	2
As 1937			20	8	2	2				
As 1971			156	63	-31	17				
Cr 2055	all with zero Cr	0.000	9	5	-3	0.7	0.3	0.2	1	0.2
Cr 2061			0	0.4	-7	4				
Cr 2677			-1	0.4	-8	4				
Cr 3578			1	1	0	0.2				
Ni 2216	all with zero Ni	0.000	1	0.4	NA	NA	-0.003	0.2	2	0.4
Ni 2316			8	4	NA	NA				
Ni 2320			379	222	NA	NA				
Ni 3414			-4	0.9	NA	NA				
Pb 2169	all with zero Pb	0.000	57	33	-12	10	1.7	0.8	7	1
Pb 2203			20	5	1	2				
Pb 2614			-309	187	-244	173				
Pb 2833			25	14	39	12				
Pd 2488	all with zero Pd	0.000	376	155	-33	12	0.8	0.4	0.8	1
Pd 3242			1	2	9	5				
Pd 3404			7	2	-5	1				
Pd 3634			322	97	43	13				

*A PE-Optima MSF model was not available for Ni

Table VI. 3σ detection limits for elements not experiencing carryover

Element	PE-Optima Univariate	PE-Optima MSF*	MWCLS-12 (12 Elements in Calibration)	MWCLS-1 (1 Element in Calibration)
	Range of Detection limits (3σ) (ng/g)	Range of Detection limits (3σ) (ng/g)	Detection limit (3σ) (ng/g)	Detection limit (3σ) (ng/g)
Aluminum (Al)	29 - 195	14 - 1066	6	7
Arsenic (As)	132 - 2363	36 - 1569	15	42
Chromium (Cr)	5 - 91	4 - 67	3	3
Nickel (Ni)	6 -3652	NA	3	8
Lead (Pb)	90 -3072	31 - 2838	15	27
Palladium (Pd)	25 - 2540	23 - 216	8	19

*A PE-Optima MSF model was not available for Ni

FIGURE CAPTIONS

1. ICP-AES spectra of all calibration and validation samples plotted vs. pixel number.
2. Peak intensity of the Cu emission at 324 nm as a function of time during and after multiple introductions of a sample containing 100 μg/g of Cu for operating conditions where the ICP auxiliary Ar flow rates are 0.5 (crosses, dashed line) and 1.0 (squares, solid line) L/min. Emission intensities are offset corrected.
3. Spectra for all 12 of the pure-element standards at ~100 μg/g in the three spectral windows specific for As at 189.0 nm, 193.7 nm, and 197.2 nm. A) All spectra and windows are at the same intensity scale so that the As bands are observed near full intensity. B) Same spectra in 3A but all spectra are scale expanded by the same factor. Dashed vertical lines separate the three As windows.
4. A) The spectra of Sample 5 (see Table I) with As at 1.00 μg/g and containing a Pt impurity at 4 μg/g that was not included in the calibration model. B) The CLS least-squares spectral residuals in each window when 12 elements (excluding Pt) are included in the model for each window. C) Alternate presentation of the spectral residuals for Sample 5 using 12 elements in the calibration model but not including the Pt impurity. Here the spectral residuals are calculated by subtracting from the sample spectrum the product of the final MWCLS concentration estimates for the 12 calibration elements and their respective CLS-estimated pure-element spectra. Dashed vertical lines separate the three As windows.

5. MWCLS-predicted Al concentrations vs. reference Al concentrations for all validation samples with Al at concentrations ranging from 0 to 300 μg/g. These samples contain as many as 11 other elements at a variety of levels from 0 to 150 μg/g.

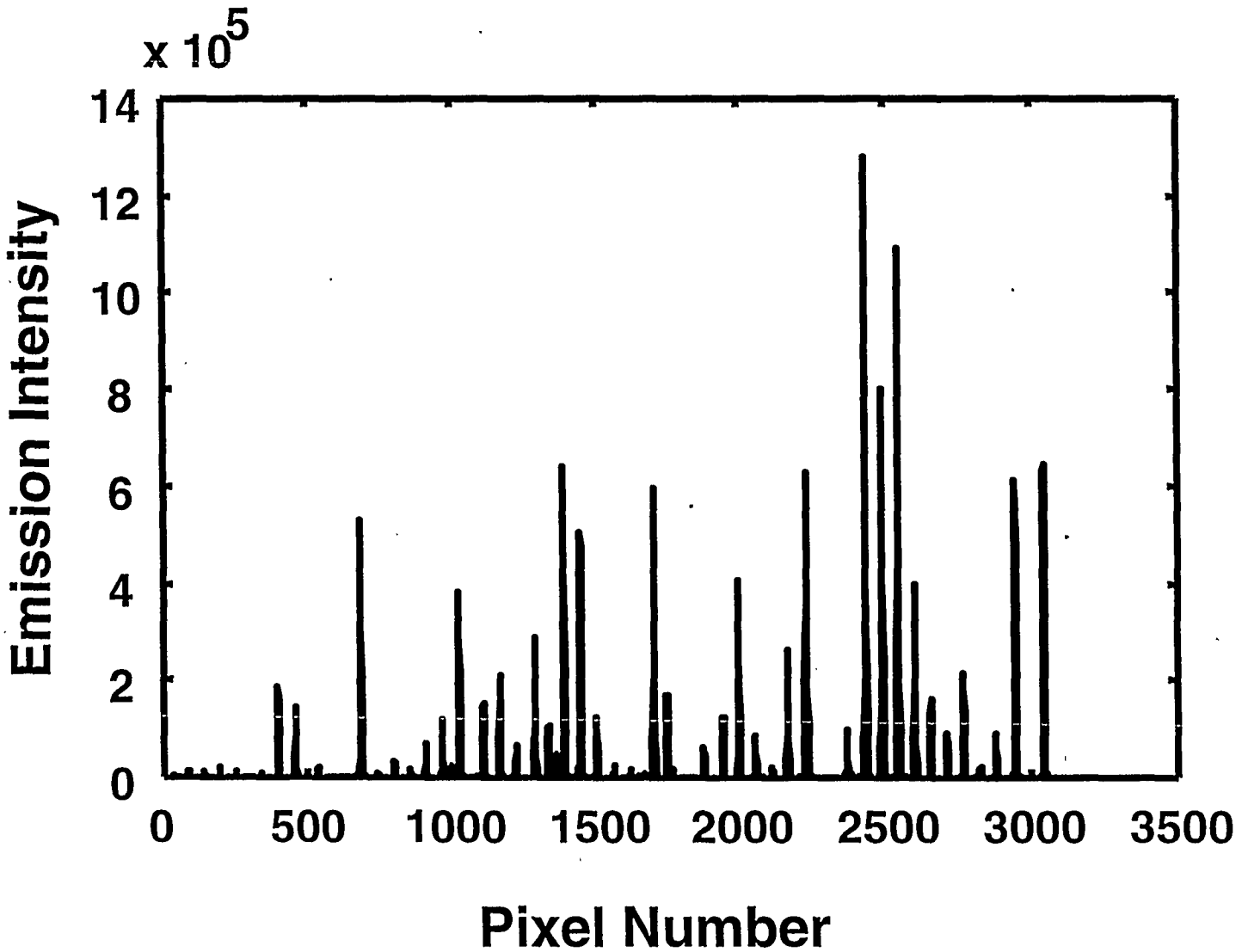
x 10^5
14
12
10
8
6
4
2
0
Emission Intensity
0
500
1000
1500
2000
2500
3000
3500
Pixel Number

Figure 1

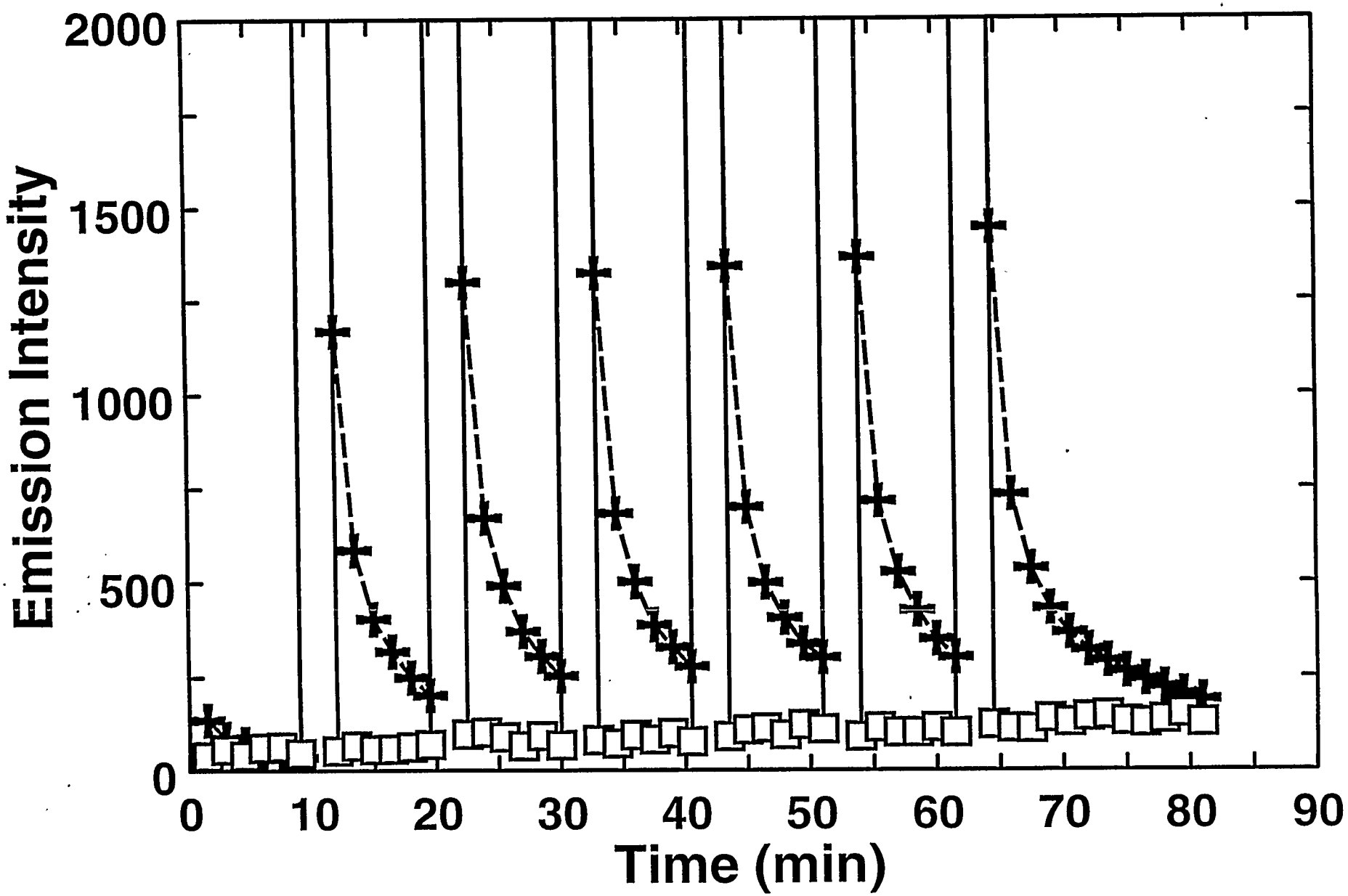
2000
1500
1000
500
0
Emission Intensity
0
10
20
30
40
50
60
70
80
90
Time (min)

Figure 2

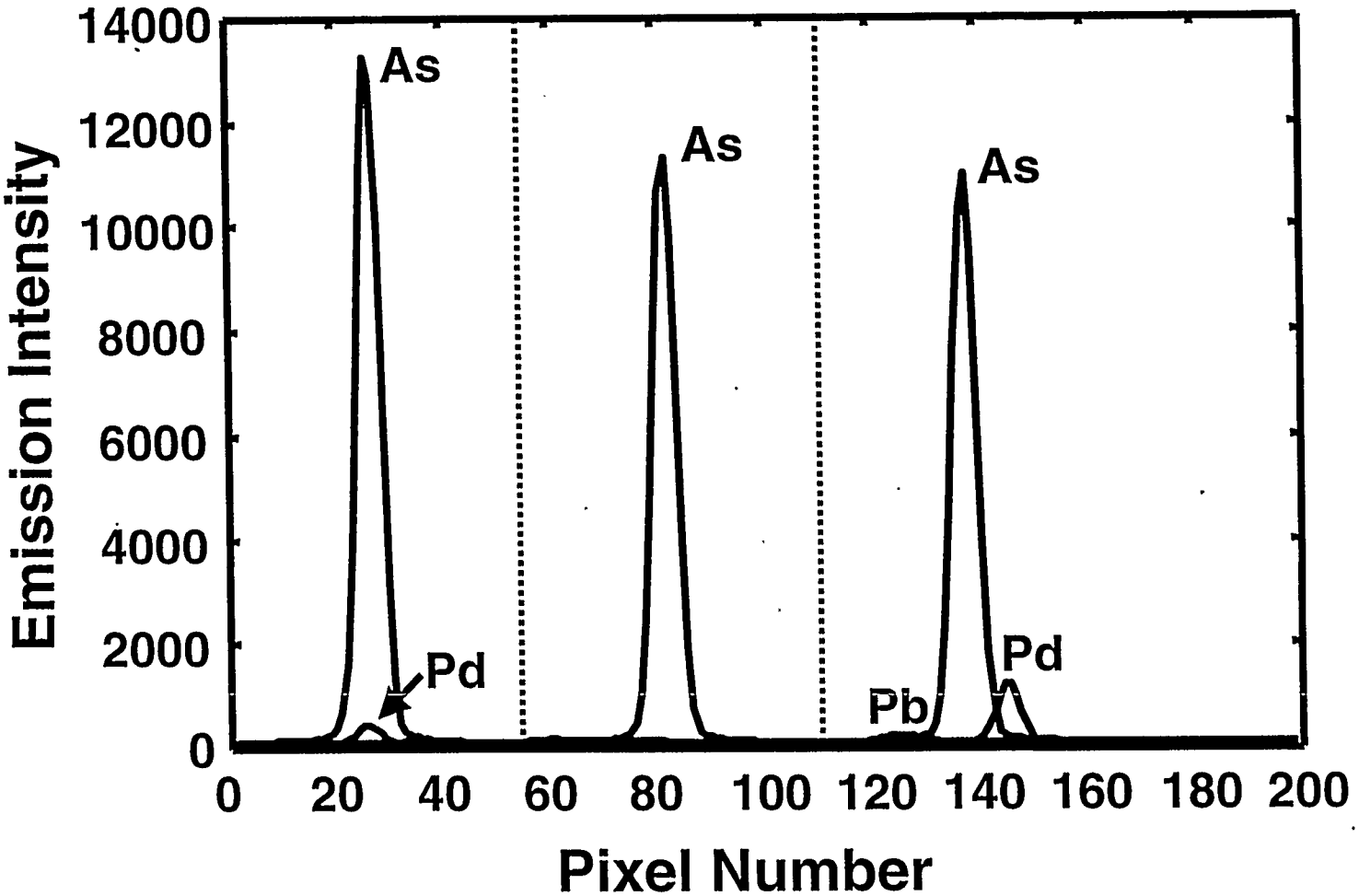
Emission Intensity
14000
12000
10000
8000
6000
4000
2000
0
As
As
As
Pd
Pb
Pd
0
20
40
60
80
100
120
140
160
180
200
Pixel Number

Figure 3A

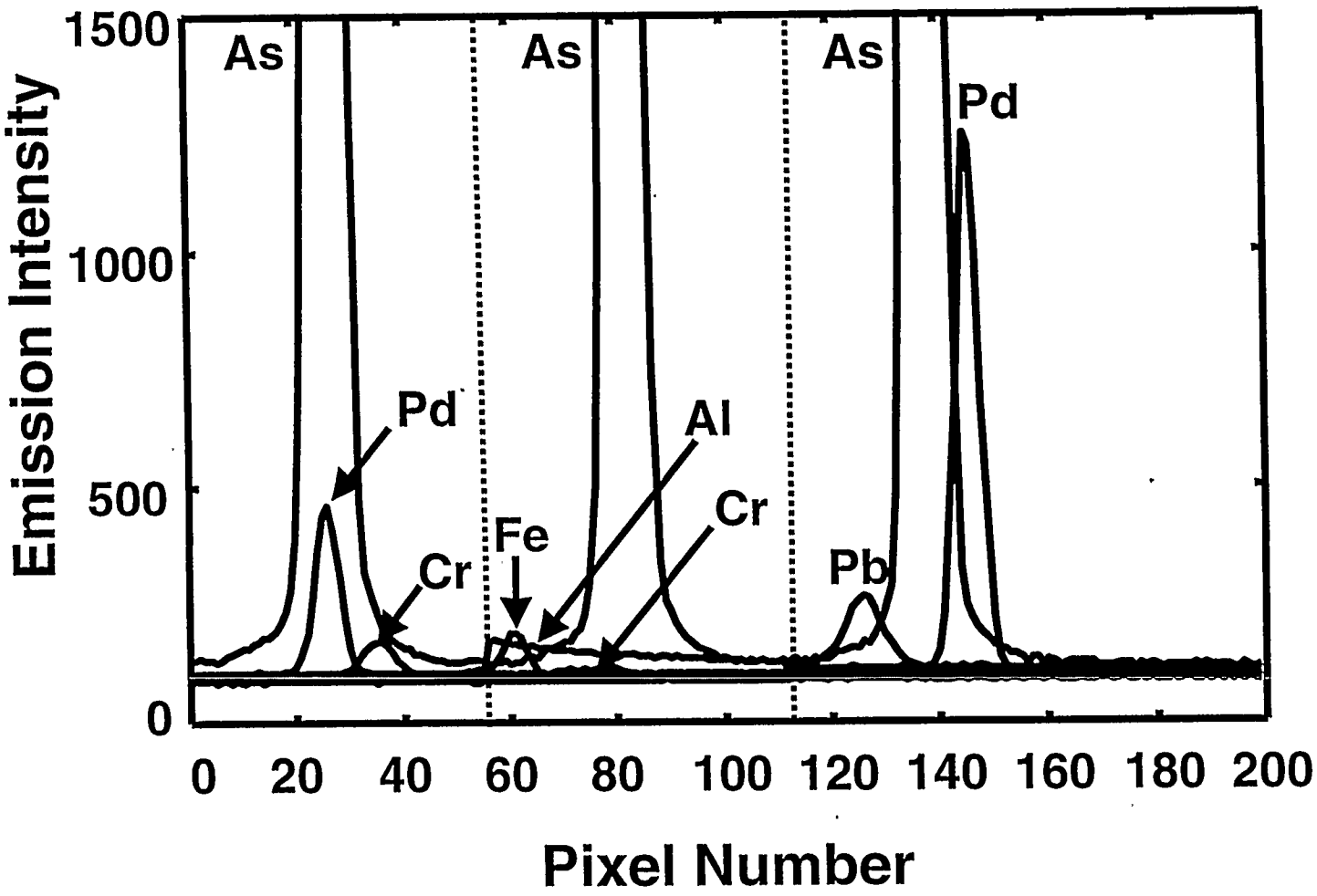
Emission Intensity
1500
1000
500
0
As
As
As
Pd
Pd
Cr
Fe
Al
Cr
Pb
0
20
40
60
80
100
120
140
160
180
200
Pixel Number

Figure 3B

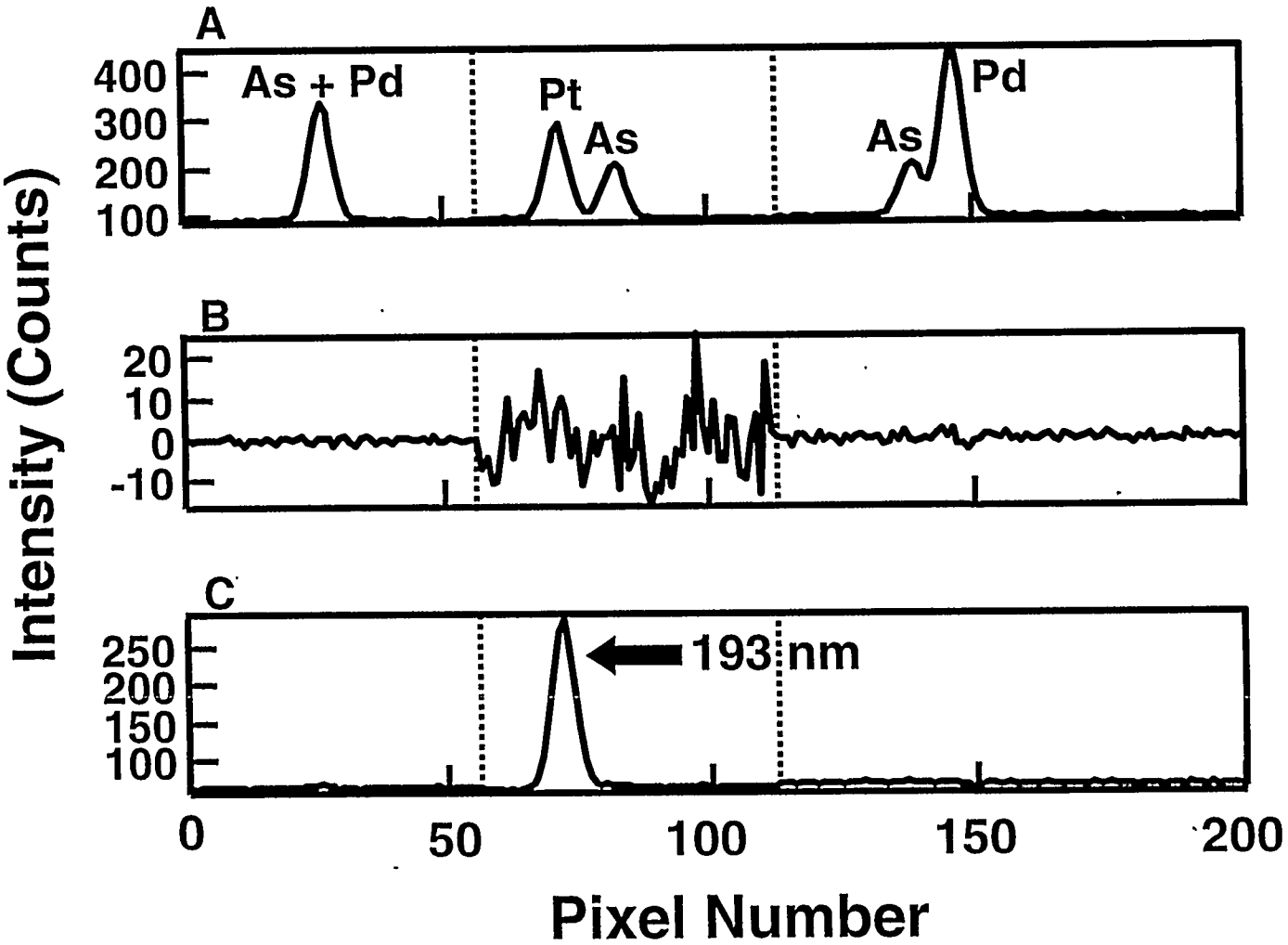
A
400
300
200
100
As + Pd
Pt
As
As
Pd
B
20
10
0
-10
C
250
200
150
100
193 nm
0
50
100
150
200
Intensity (Counts)
Pixel Number

Figure 4

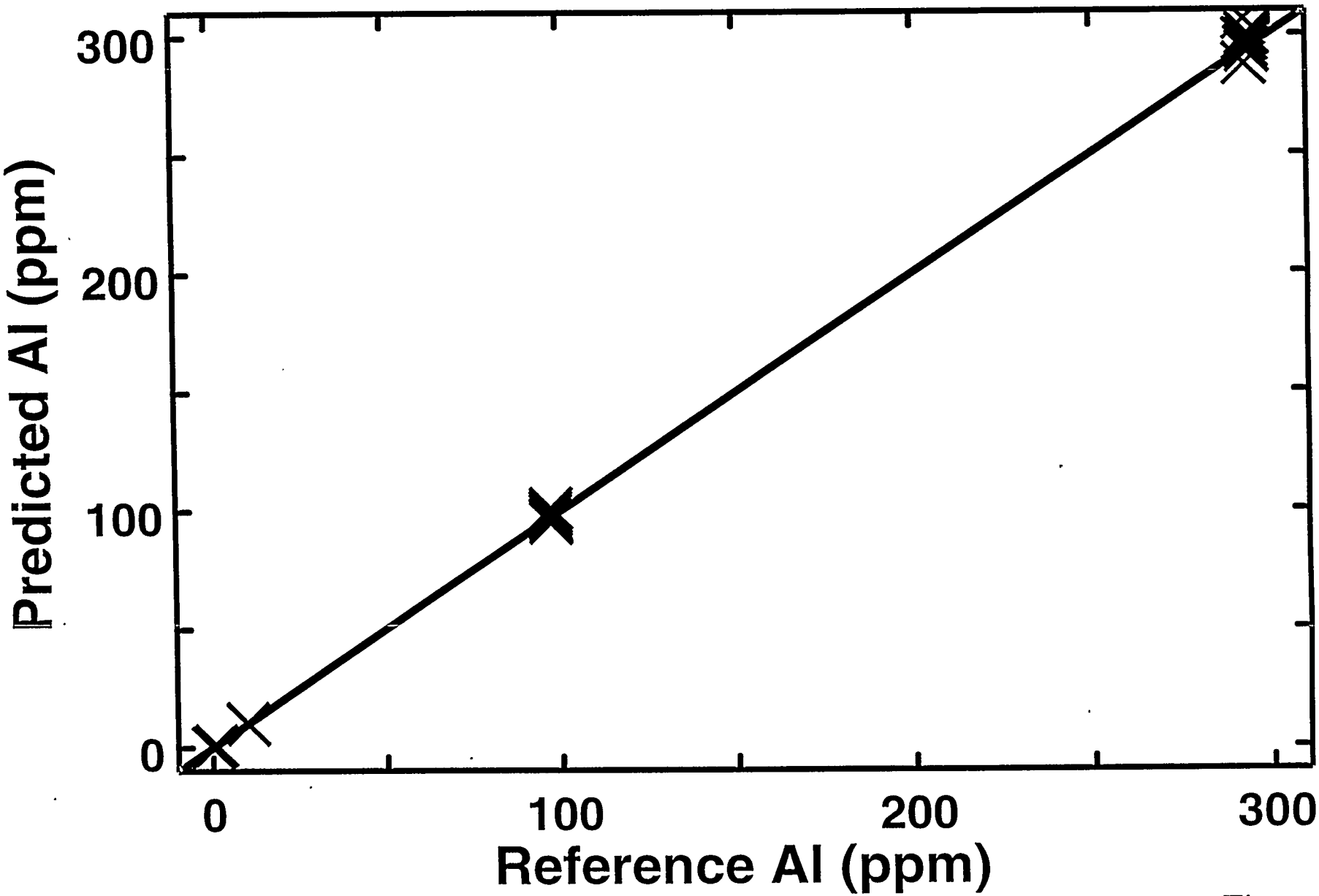

Figure 5